

Measurements of X_{\max} above 10^{17} eV with the fluorescence detector of the Pierre Auger Observatory

Alessio Porcelli^{*,a} for the Pierre Auger Collaboration^b

^aKarlsruhe Institute of Technology, Karlsruhe, Germany,
currently at the Department of Nuclear Physics, University of Geneva, Geneva, Switzerland

^bObservatorio Pierre Auger, Av. San Martín Norte 304, 5613 Malargüe, Argentina

E-mail: auger_spokespersons@fnal.gov

Full author list: http://www.auger.org/archive/authors_2015_06.html

For the first time the Pierre Auger Collaboration presents $\langle X_{\max} \rangle$ and $\sigma(X_{\max})$ measurements covering nearly three decades of energy. In this analysis we include new X_{\max} data obtained with the High Elevation Auger Telescopes (HEAT) enhancement. The HEAT telescopes cover a field of view ranging from 30° to 60° of elevation and are located next to one of the standard fluorescence detector sites (Coihueco). The combination of the HEAT and Coihueco telescopes covers a field of view from $\sim 2^\circ$ up to $\sim 60^\circ$ of elevation. Thus, the combination can sample the longitudinal profile of nearby lower energy showers, allowing us to extend the energy range down to 10^{17} eV.

*The 34th International Cosmic Ray Conference,
30 July- 6 August, 2015
The Hague, The Netherlands*

*Speaker.

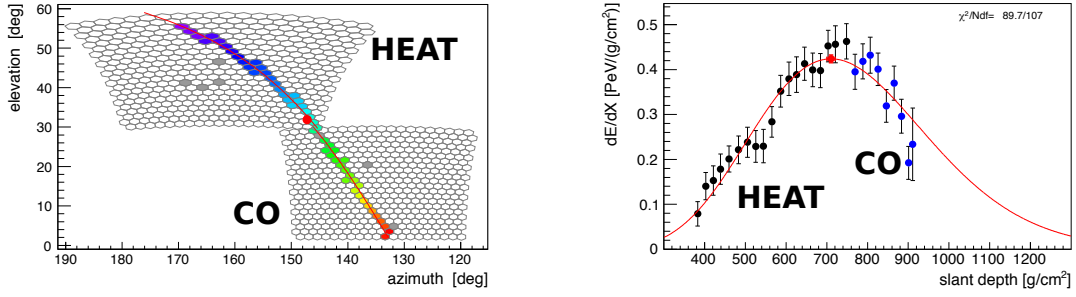


Figure 1: Example of a HeCo event with an energy of $(3.7 \pm 0.1) \times 10^{17}$ eV. Left: the camera view, the timing of the pixel pulses is color-coded (early = blue, late = red). Right: the measured longitudinal profile (black dots — HEAT, blue dots — Coihueco) with the Gaisser-Hillas fit (red line). The red point in both panels indicates the X_{\max} position.

1. Introduction

The knowledge of the composition of cosmic rays in the energy range of 0.1 to 1 EeV is a key ingredient to identify a possible transition from galactic to extra-galactic sources and for understanding the nature of the energy spectrum features (ankle at ≈ 4 EeV and cut-off at ≈ 40 EeV).

The depth at which the number of secondary air-shower particles reaches its maximum, X_{\max} , is one of the most robust observables for studying the mass composition [1]. Experimentally, the longitudinal profile of the shower development can be measured using fluorescence light emitted by molecules of atmospheric nitrogen excited by Extensive Air Shower (EAS) particles. At the Pierre Auger Observatory, which is continuously taking data since 01.2004, such measurements are performed using the fluorescence detector (FD) consisting of 24 telescopes placed at 4 locations and, since 06.2010, using the High Elevation Auger Telescopes (HEAT). With these telescopes the Field of View (FoV) of the Coihueco (CO) site is expanded from $2 \div 30^\circ$ up to $2 \div 60^\circ$ of elevation, which allows one to observe nearby low energy showers ($E < 10^{17.8}$ eV). In Figure 1 an example of a low energy event in the enlarged FoV is shown: the track on the camera (left) and the longitudinal profile with the Gaisser-Hillas fit (right).

The determination of the primary composition with FD data is performed using the characteristics of measured X_{\max} distributions of EAS. The first two moments of the X_{\max} distribution ($\langle X_{\max} \rangle$ and $\sigma(X_{\max})$) are related to the first two moments of the distribution of the logarithm of masses of primary particles ($\ln A$ and $\sigma(\ln A)$) [2]:

$$\langle X_{\max} \rangle = \langle X_{\max} \rangle_p + f_E \langle \ln A \rangle \quad (1.1)$$

$$\sigma^2(X_{\max}) = \langle \sigma_{sh}^2 \rangle + f_E^2 \sigma^2(\ln A). \quad (1.2)$$

$\langle X_{\max} \rangle_p$ and $\langle \sigma_{sh}^2 \rangle$ are the mean X_{\max} for protons and the composition-averaged shower-to-shower fluctuations¹, and f_E is a parameter depending on details of hadronic interactions, properly parametrized from the interaction models for energies $\geq 10^{17}$ eV.

¹ $\langle \sigma_{sh}^2 \rangle = \sum_i f_i \sigma_i^2(X_{\max})$ where f_i is the relative fraction of mass A_i

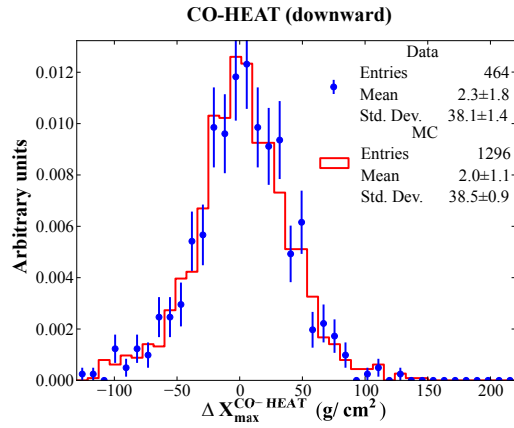


Figure 2: X_{\max} difference between CO and HEAT (in downward mode) in MC simulation (red histogram) and data (blue dots).

In this paper, nearly two years of calibrated HEAT data, from 01.06.2010 to 15.08.2012, are used to extend the previous measurement of the X_{\max} moments [1] from $10^{17.8}$ eV down to 10^{17} eV.

2. Data analysis

The analysis presented in this paper is based on two datasets. The data collected by the standard FD telescopes during the period from 01.12.2004 to 31.12.2012 (published in [1]), and the data collected with HEAT and Coihueco telescopes (HeCo) during the period from 01.06.2010 to 15.08.2012.

HEAT can be operated in upward and downward modes. The downward mode is when the telescopes are oriented such that their elevation angle extends up to 30° (same as the standard Auger telescopes). The upward mode is when they cover an elevation angle ranging from 30° to 60° (this is the HEAT standard operation mode). The HEAT downward mode is used for systematic cross checks, because it allows one to observe the same showers in coincidence with telescopes from the Coihueco site. In Figure 2 the X_{\max} difference between CO and HEAT in downward mode is shown. Data (blue dots) and simulations (red lines) are in agreement, which implies a good knowledge of the detector.

The standard FD dataset contains events with energies above $10^{17.8}$ eV and the HeCo one contains events with energies above $10^{17.0}$ eV. HeCo runs out of statistics at energies beyond $E < 10^{18.3}$ eV. In order to combine two statistically independent datasets, we have removed from the standard FD dataset all Coihueco events with energies below $E < 10^{18.3}$ eV and recorded during the HeCo period (from 01.06.2010 to 15.08.2012). This cut has reduced the standard FD data by only 1377 events (out of 19759 events).

2.1 Data selection

The analysis is based on hybrid events, i.e. on events with geometries reconstructed using information on arrival times of both light in the cameras of FD telescopes and of the shower front at ground as measured by the ground station closest to the shower axis. We selected data recorded

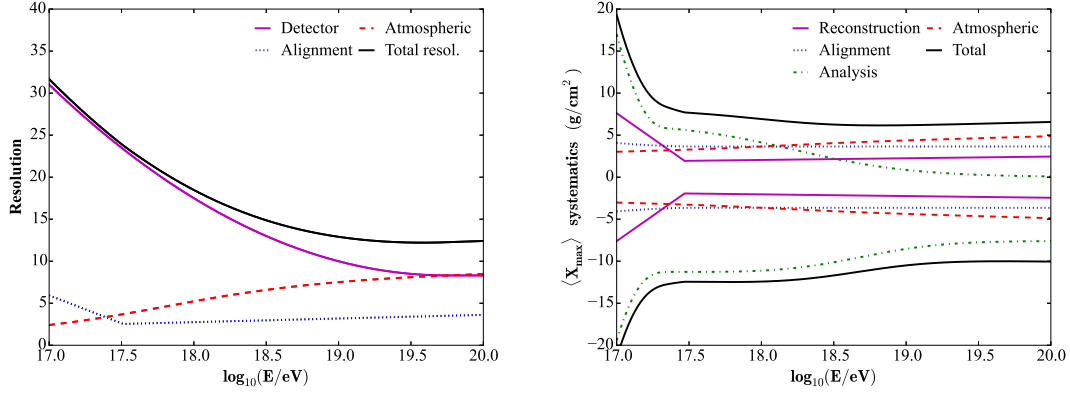


Figure 3: X_{\max} resolution (left) and systematic uncertainties in the X_{\max} scale (right) as functions of energy.

during stable running conditions and good atmospheric conditions [1]. In addition to these selection criteria a set of fiducial FoV cuts are applied to reduce to the minimum the detector effects in the sampled X_{\max} distributions (as explained in Section 2.2).

For the HeCo dataset, specific corrections to $\langle X_{\max} \rangle$ and $\sigma(X_{\max})$ are applied to reduce residual biases, especially for the lower energy bins ($E < 10^{17.5}$ eV).

2.2 FoV selection criteria

A shower is reconstructed accurately only if its X_{\max} is within the FoV. Shallow or deep events are more likely to have their X_{\max} values outside the FoV and have larger chances to be excluded from the analysis. In general, at the lower energies where the showers are closer to the telescopes, the limited FoV biases the sample towards lighter composition (i.e. towards deeper X_{\max} values).

For data satisfying the selection criteria explained in Section 2.1, a fiducial FoV is derived. This fiducial range is characterized by the lower X_{low} and upper X_{up} boundaries. These parameters define the slant depth range where X_{\max} of each event would be reconstructed with a resolution better than 40 g cm^{-2} . To have higher quality events, the X_{\max} value must fall inside these boundaries. Furthermore, if the values of X_{low} and X_{up} are not within certain limits (i.e. X_{low} and X_{up} should enclose the bulk of the X_{\max} distribution), the event is also excluded.

The processes to calculate X_{low} and X_{up} parameters, and the limits on them, are explained in detail in [1].

2.3 Estimating the X_{\max} moments

After the application of all selection criteria, the moments of the X_{\max} distribution are estimated as described in [1]. Reconstruction and residual acceptance biases are estimated through simulations and corrected for. The observed width of the distribution is corrected by subtracting the detector resolution (Figure 3, left) in quadrature to obtain $\sigma(X_{\max})$.

The systematic uncertainty in the X_{\max} scale is displayed in Figure 3 (right). At low energies it is dominated by uncertainties of the analysis procedure, at high energies atmospheric uncertainties give as well a significant contribution.

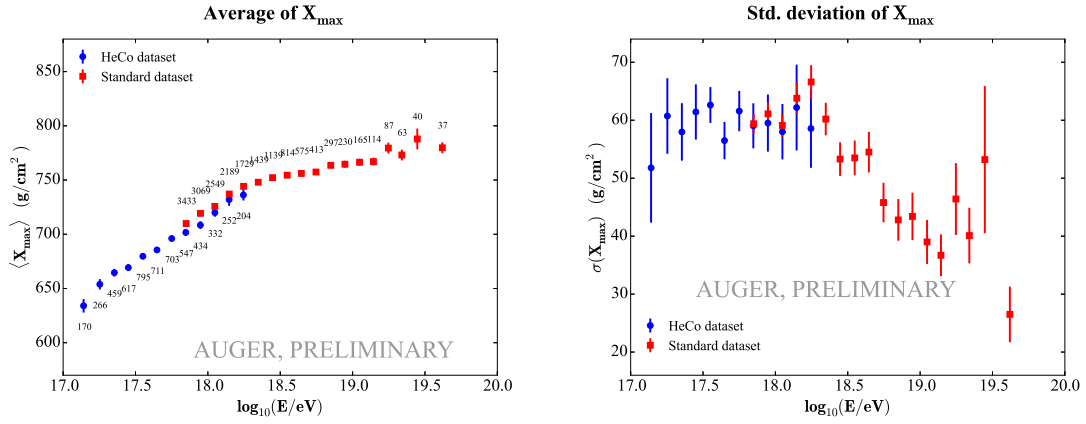


Figure 4: The mean (left) and standard deviation (right) of measured X_{\max} distributions of the two independent datasets: HeCo (blue circles) and the standard FD (red squares).

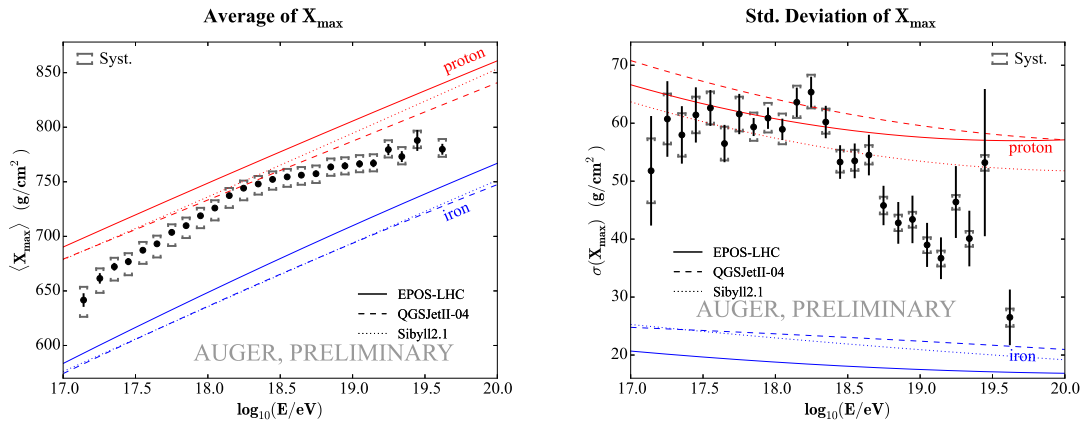


Figure 5: The mean (left) and the standard deviation (right) of the measured X_{\max} distributions (combining HeCo and standard datasets) as a function of energy compared to air-shower simulations for proton and iron primaries.

2.4 Results and Interpretation

In Figure 4 the X_{\max} moments estimated using HeCo and the standard FD datasets are compared. While $\langle X_{\max} \rangle$ differs by $\sim 7 \text{ g cm}^{-2}$ between datasets (within the uncorrelated systematics of the two analyses), the second moments $\sigma(X_{\max})$ are found to be in a good agreement. For the combination of the datasets the HeCO $\langle X_{\max} \rangle$ is shifted by $+7 \text{ g cm}^{-2}$ and the resulting $\langle X_{\max} \rangle$ and $\sigma(X_{\max})$ are shown in Figure 5.

Between $10^{17.0}$ and $10^{18.3}$ eV $\langle X_{\max} \rangle$ increases by around 85 g cm^{-2} per decade of energy (Figure 5, left). This value, being larger than the one expected for a constant mass composition ($\sim 60 \text{ g cm}^{-2}/\text{decade}$), indicates that the mean primary mass is getting lighter. Around $\approx 10^{18.3}$ eV the observed rate of change of $\langle X_{\max} \rangle$ becomes significantly smaller ($\sim 26 \text{ g cm}^{-2}/\text{decade}$) indicating that the composition is becoming heavier. The fluctuations of X_{\max} (Figure 5, right) start to decrease at around the same energy $\approx 10^{18.3}$ eV.

The mean value of $\ln A$ and its variance $\sigma^2(\ln A)$, determined from Equations (1.1) and (1.2),

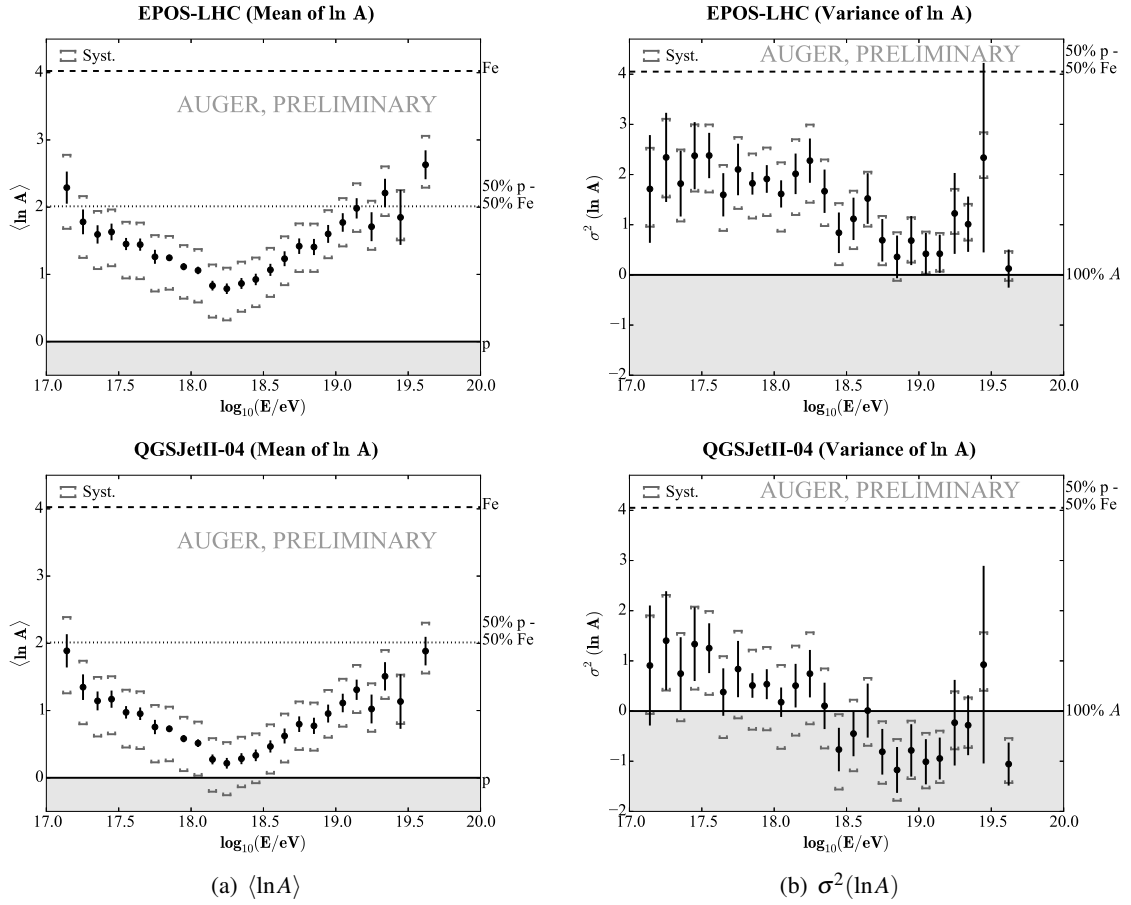


Figure 6: The mean (left) and the variance (right) of $\ln A$ estimated from data with EPOS-LHC (up) and QGSJetII-04 (down).

are shown in Figure 6. For the parameters $\langle X_{max} \rangle_p$, f_E and $\langle \sigma_{sh}^2 \rangle$, EPOS-LHC and QGSJetII-04 hadronic interaction models are used.

For both models the similar trends with energy for $\langle \ln A \rangle$ and $\sigma^2(\ln A)$ are observed. The primary mass is decreasing reaching the minimal values at around $10^{18.3}$ eV and starts to increase for the higher energies. The spread of the masses is almost constant till $\approx 10^{18.3}$ eV and then starts to decrease, together with the behavior of $\langle \ln A \rangle$ that might be an indication that the relative fraction of protons becomes smaller for the energies above $\approx 10^{18.3}$ eV (see [3]).

References

- [1] The Pierre Auger Collaboration, *Depth of Maximum of Air-Shower Profiles at the Pierre Auger Observatory: Measurements at Energies above $10^{17.8}$ eV*, *Phys.Rev. D90* **12** (2014) 122005, [1409.4809v3].
- [2] The Pierre Auger Collaboration, *Interpretation of the Depths of Maximum of Extensive Air Showers Measured by the Pierre Auger Observatory*, *JCAP* **1302** (2013) 026, [1301.6637v2].
- [3] The Pierre Auger Collaboration, *Depth of maximum of air-shower profiles at the Pierre Auger Observatory. II. Composition implications*, *Phys.Rev. D90* **12** (2014) 122006, [1409.5083v1].